Biochimica et Biophysica Acta 1838 (2014) 2728–2738

Contents lists available at ScienceDirect

Biochimica et Biophysica Acta

journal homepage: www.elsevier.com/locate/bbamem

Galleria mellonella native and analogue peptides Gm1 and ΔGm1. I) Biophysical characterization of the interaction mechanisms with bacterial model membranes

Wilmar Correa [a], Marcela Manrique-Moreno [a], Edwin Patiño [a], Carlos Peláez-Jaramillo [a], Yani Kaconis [b], Thomas Gutsmann [b], Patrick Garidel [c], Lena Heinbockel [b], Klaus Brandenburg [b,*]

[a] *Instituto de Química, Facultad de Ciencias Exactas y Naturales, Universidad de Antioquia, AA. 1226 Medellín, Colombia*
[b] *Forschungszentrum Borstel, LG Biophysik, D-23845 Borstel, Germany*
[c] *Martin-Luther-University Halle/Wittenberg, Department of Chemistry/Physical Chemistry, D-06120 Halle/Saale, Germany*

ARTICLE INFO

Article history:
Received 22 October 2013
Received in revised form 29 April 2014
Accepted 1 July 2014
Available online 10 July 2014

Keywords:
Antimicrobial peptide
Peptide–lipid interaction
Lipopolysaccharide
Cell membrane
Attenuated total reflection
Differential scanning calorimetry

ABSTRACT

Natural occurring antimicrobial peptides (AMPs) are important components of the innate immune system of animals and plants. They are considered to be promising alternatives to conventional antibiotics. Here we present a comparative study of two synthetic peptides: Gm1, corresponding to the natural overall uncharged peptide from Galleria mellonella (Gm) and ΔGm1, a modified overall positively charged Gm1 variant. We have studied the interaction of the peptides with lipid membranes composed of different kinds of lipopolysaccharides (LPS) and dimyristoylphosphatidylglycerol (DMPG), in some cases also dimyristoylphosphatidylethanolamine (DMPE) as representative lipid components of Gram-negative bacterial membranes, by applying Fourier-transform infrared spectroscopy (FTIR), Förster resonance energy transfer spectroscopy (FRET), differential scanning calorimetry (DSC) and isothermal titration calorimetry (ITC). Gm1 generates a destabilizing effect on the gel to liquid crystalline phase transition of the acyl chains of the lipids, as deduced from a decrease in the phase transition temperature and enthalpy, suggesting a fluidization, whereas ΔGm1 led to the opposite behavior. Further, FTIR analysis of the functional groups of the lipids participating in the interaction with the peptides indicated a shift in the band position and intensity of the asymmetric PO_2^- stretching vibration originating from the lipid phosphate groups, a consequence of the sterical changes in the head group region. Interestingly, FRET spectroscopy showed a similar intercalation of both peptides into the DMPG and LPS, but much less into the DMPE membrane systems. These results are discussed in the light of a possible use of the peptides as antimicrobial and anti-endotoxin drugs.

1. Introduction

The ability of bacterial pathogens to accumulate mutations leading to resistance and the excessive use of antibiotics in therapy have led to an increase of multidrug-resistant microbes which represent a new challenge in the treatment of infectious diseases today [1]. Another frequent disadvantage of traditional antibiotics is the release of lipopolysaccharides (LPS) from the outer membrane of Gram-negative bacteria during cell lysis. LPS is one of the most potent activators of the human immune system, which may lead to severe inflammation [2]. Natural occurring antimicrobial peptides (AMPs) are important components of the innate immune system of animals and plants [3]. Most AMPs are small molecules consisting of 10–50 amino acids with an amphipathic secondary structure which are positively charged at physiological conditions and are thought to act by a rapid destruction of bacterial membranes [4–6]. AMPs have been conserved throughout the evolution process because the disruption of these membranes leads to

Abbreviations: AMPs, Antimicrobial peptides; Gm, *Galleria mellonella*; DMPG, dimyristoylphosphatidylglycerol; DMPE, dimyristoylphosphatidylethanolamine; FTIR, Fourier-transform infrared spectroscopy; FRET, Förster resonance energy transfer spectroscopy; DSC, differential scanning calorimetry; ITC, isothermal titration calorimetry; LPS, lipopolysaccharides; PBS, phosphate buffer saline; NBD-PE, NBD-phosphatidylethanolamine; Rh-PE, Rhodamine-PE; ATR, attenuated total reflection; T_m, main transition temperature; P_{β}, ripple phase; L_{β}, gel phase; L_{α}, liquid crystalline phase; *E. coli*, *Escherichia coli*; LMVs, large multilamellar vesicles

* Corresponding author at: Forschungszentrum Borstel, Laborgruppe Biophysik, Parkallee 10, 23845 Borstel, Germany. Tel.: +49 4537 188235; fax: +49 4537 188632.
E-mail addresses: wilcova@gmail.com (W. Correa), mmanriqm@exactas.udea.edu.co (M. Manrique-Moreno), epatino@matematicas.udea.edu.co (E. Patiño), directorgiem@gmail.com (C. Peláez-Jaramillo), ykaconis@fz-borstel.de (Y. Kaconis), tgutsmann@fz-borstel.de (T. Gutsmann), Patrick.Garidel@chemie.uni-halle.de (P. Garidel), lheinbockel@fz-borstel.de (L. Heinbockel), kbrandenburg@fz-borstel.de (K. Brandenburg).

http://dx.doi.org/10.1016/j.bbamem.2014.07.006
0005-2736/

rapid bacterial killing with a low potential for the development of resistances. Furthermore they are considered to be promising alternatives to conventional antibiotic treatment, because they exhibit a broad spectrum of antimicrobial activity against fungi, bacteria and protozoa [7]. Also referred as host-defense peptides they have been of increasing interest in recent years as potent new anti-infectives [3,8,9]. An understanding of the mechanism of AMPs with bacterial membranes is fundamental for explaining the biological activity of these peptides and for developing new compounds with optimized biological activities [10].

It was found that each insect species can express an individual set of antimicrobial peptides in response to invading microorganisms, which may also exert anti-endotoxin activity [11,12]. To defend itself against invading microbes, *Galleria mellonella* (*G. mellonella*) concurrently releases an impressive array of at least 18 known or putative antimicrobial peptides from 10 families. The peptides were investigated by LC/MS and gene expression analyses [13]. Other studies of this biological model revealed a different response depending on the kind of infection [14–16]. Gm cecropin D-like peptide (Gm1), a native overall uncharged peptide obtained from *G. mellonella* [17], is the peptide with the broadest activity spectrum, with proven activity against different kinds of Gram-positive bacteria and *Escherichia coli* (*E. coli*) D31 as well as filamentous fungi. Therefore, Gm1 is a promising candidate peptide for elucidating its biophysical mechanism in order to further characterize it and to evaluate its ability to neutralize the endotoxic properties of LPS components of the outer membrane of Gram-negative bacteria [18].

Here, we present a comparative systematic study of two synthetic peptides: Gm1 and ΔGm1, a modified structure of Gm1 which is overall positively charged with a change of 5 amino acids compared to Gm1. We have studied the interaction of these peptides with model membranes by applying Förster-resonance energy transfer spectroscopy (FRET) in order to elucidate the intercalation of peptides into lipid membranes consisting of LPS R60 and DMPG as representative of negatively charged components of Gram-negative bacteria membranes [19,20]. Fourier-transform infrared spectroscopy (FTIR) as a useful tool was applied for studying lipid–peptide interactions, by characterizing the gel to liquid crystalline phase transitions of the lipids and the binding epitopes within the lipid head groups and by analyzing the secondary structures of the peptides.

2. Materials and methods

2.1. Peptides

Peptides were synthesized without amidated C-terminus by Fmoc solid-phase synthesis technique with an automatic peptide synthesizer (433 A Applied Biosystems Synthesizer) in Head-Clinical Tumor Proteomics Facility-CTPF-Lausanne Cancer Center, Switzerland. The net charge (Q) of the peptides was calculated by subtracting the number of aspartic (D) and glutamic (E) acid residues (the negatively charged amino acid residues present in the peptides) from all positive charges (lysine, arginine and the peptide's N-terminus). The hydrophobicity plots were made using the consensus scale of hydrophobicity proposed by Eisenberg et al. [21].

2.2. Lipids and reagents

Rough type lipopolysaccharides (LPS) of *Salmonella enterica* (serovar Minnesota) R595 and R60 and from *Proteus mirabilis* R45 (polymyxin B-resistant) were extracted by using the phenol/chloroform/petrol ether method. Bacterial cultures were grown at 37 °C and LPS was purified and lyophilized as described before [22]. The phospholipids dimyristoylphosphatidylglycerol (DMPG) and dimyristoylphosphatidylethanolamine (DMPE) were purchased from Avanti Polar Lipids. NBD-phosphatidylethanolamine (NBD-PE) and rhodamine-PE (Rh-PE) were purchased from Molecular Probes (Eugene, OR, U.S.A.). All other chemicals were acquired from Merck.

2.3. Lipid sample preparation

The phospholipids and LPS samples were prepared as aqueous dispersions in buffer (20 mM HEPES pH 7.4). The lipid concentrations ranged from 1 to 20 mM, depending on the sensitivity of the applied technique. In all cases, the lipids were suspended directly in buffer by extensive mixing, sonicated in a water bath at 60 °C for 30 min, cooled down to 5 °C and subjected to three cycles of heating and cooling from 60 °C to 5 °C. After that the lipid samples were stored for at least 24 h at 4 °C before performing the measurements.

2.4. Fourier-transform infrared spectroscopy (FTIR)

The infrared spectroscopic measurements were performed on an IFS-55 spectrometer (Bruker, Karlsruhe, Germany). For phase transition measurements, pure lipids suspended in 20 mM HEPES buffer (pH 7.4) as well as lipids mixed with peptides solubilized in the same buffer at molar ratios from 1:0.0 to 1:1.0 were placed in a CaF_2 cuvette with a 12.5 μm Teflon spacer. Consecutive heating scans were performed automatically from 10 °C to 70 °C with a heating rate of 0.6 °C min^{-1}. Every 3 °C, 200 interferograms were accumulated, apodized, Fourier transformed, and converted to absorbance spectra. The peak position of the asymmetric stretching vibration of the methylene band $\nu_s(CH_2)$ sensitive marker lipid order [23] was plotted versus temperature. Phase transition temperatures were derived by determination of the maximum of the first derivative of the heating scans.

For measurement of hydrated lipids, samples were spread on an attenuated total reflectance (ATR) ZnSe crystal and free water was evaporated under a stream of N_2. Vibrational bands from the interface region (1700–1750 cm^{-1}), amide I (1600–1700 cm^{-1}) and head groups (1000–1300 cm^{-1}) were analyzed in order to study the membrane: peptide interaction. The instrumental wavenumber resolution was better than 0.02 cm^{-1}, the wavenumber reproducibility in repeated scans was better than 0.1 cm^{-1}.

2.5. Differential scanning calorimetry

Calorimetry measurements were performed with a VP-DSC calorimeters (MicroCal Inc., Northampton, MA, USA) at a heating and cooling rate of 1 $K \cdot min^{-1}$ as described [24]. The DSC samples were prepared by dispersing a known ratio of lipid to the peptide in 10 mM PBS (phosphate buffered saline, 10 mM phosphate, 138 mM NaCl, 2.7 mM KCl) buffer at pH 7.4. The samples were hydrated in the liquid crystalline phase by mixing thoroughly.

The measurements were performed in the temperature interval from 5 °C to 95 °C. In the figures, only the temperature range at which phase transitions were observed is shown. Five consecutive heating and cooling scans checked the reproducibility of the DSC experiments of each sample. The accuracy of the DSC experiments was ±0.1 °C for the main phase transition temperatures and ± 1 kJ/mol for the main phase transition enthalpy [25]. The DSC data were analyzed using the Origin software, and the phase transition enthalpy was obtained by integrating the area under the heat capacity curve.

2.6. Förster resonance energy transfer (FRET) spectroscopy

The intercalation of peptides into liposome membranes was determined in 20 mM HEPES, 150 mM NaCl, and pH 7.4, at 37 °C by FRET spectroscopy applied as a probe dilution assay [26]. The peptides were added to liposomes which were labeled with donor dye NBD-PE and acceptor dye Rh-PE. Intercalation was monitored by the increase of the ratio of donor fluorescence intensity I_D at 531 nm to acceptor intensity I_A at 593 nm in a time dependent manner. For the evaluation of the

measurements, the ratio I_D/I_A is plotted versus lipid:peptide ratio as sensitive measure of peptide intercalation into the lipid membranes.

2.7. Isothermal titration calorimetry

The binding of the peptides with DMPG liposomes or LPS-aggregates was analyzed by microcalorimetric measurements on an MCS (Microcal Inc., MA, USA) as described recently [27,28]. For this, 3 μL of 0.2 mM peptides was titrated 30 times to 1.5 mL of 0.05 mM lipid dispersions and the measured enthalpy changes were recorded versus time and concentration ratio of peptide to lipid. The heats of dilution were determined in control experiments by injecting peptide solution into buffer (20 mM HEPES, pH 7.4) and were subtracted from the heats determined in the corresponding peptide–lipid binding experiments.

The evaluation of the binding curves was done according to standard thermodynamics. Measurements were done at 37 °C.

3. Results

3.1. Design of ΔGm1 from basic Gm1 sequence

The antibacterial activity of the peptide Gm1 is well documented [16,17], however, its interaction with phospholipids and its membrane permeabilizing potency on model membranes made of different phospholipids and lipopolysaccharides have not been documented. We used Gm1 wild type to generate ΔGm1 based on the suggestion given by D. Bordo and P. Argos [29] in order to increase the number of positive charges and maintain the molecular structure. The server NCBI/BLAST (http://blast.ncbi.nlm.nih.gov) allows the analysis and comparison of primary structures of peptides. The peptide Gm1 belongs to the cecropin family of peptides and we found that the sequence AAPA is highly conserved and tends to form a loop motif. In this structure, the AAPA motif was replaced by RRPR in order to maintain the structure of the initial peptide. These changes are supported by Bryson et al. [30] who observed that the structures of two, three and four chains, in α-helical shape, acquire a loop structure when they have the sequence RRPR. Further, Ala and Arg have similar values of the change of free energy, indicating that the exchange led to the same structural patterns in peptides and proteins [31]. The amino acids Ile 7 and Ala 10 were replaced by Lys that are likely to form helical structures and to maintain positive residues on one site.

The amphipathicity of these peptides is illustrated in Fig. 1, under the assumption of an α-helical shape corroborated by the I-TASSER platform [32]. The amphipathicity of Gm1 is reflected by the segregation of hydrophilic and hydrophobic amino acid residue side chains in two structural regions, one more hydrophilic than the other one (Fig. 1A). On the other hand, ΔGm1 displays a structure more hydrophilic along the entire sequence (Fig. 1B).

3.2. Conformation of lipid head groups by FTIR spectroscopy applying attenuated total reflectance (ATR)

Infrared spectroscopy is a powerful technique to determine the conformation and orientation of membrane-associated proteins and peptides associated with lipids [33–35]. For an analysis of the band shapes, we applied a Gaussian/Lorentzian curve fitting to the original unprocessed spectra. Prior to this procedure, we identified the peak positions of the single band components by Fourier self-deconvolution and second derivatives of the FTIR spectra of the lipids and peptides.

For the elucidation of the electrostatic interactions between DMPG, LPS R60 and the peptides, vibrational bands from the lipid head groups, in particular the negatively charged phosphate groups [36], were

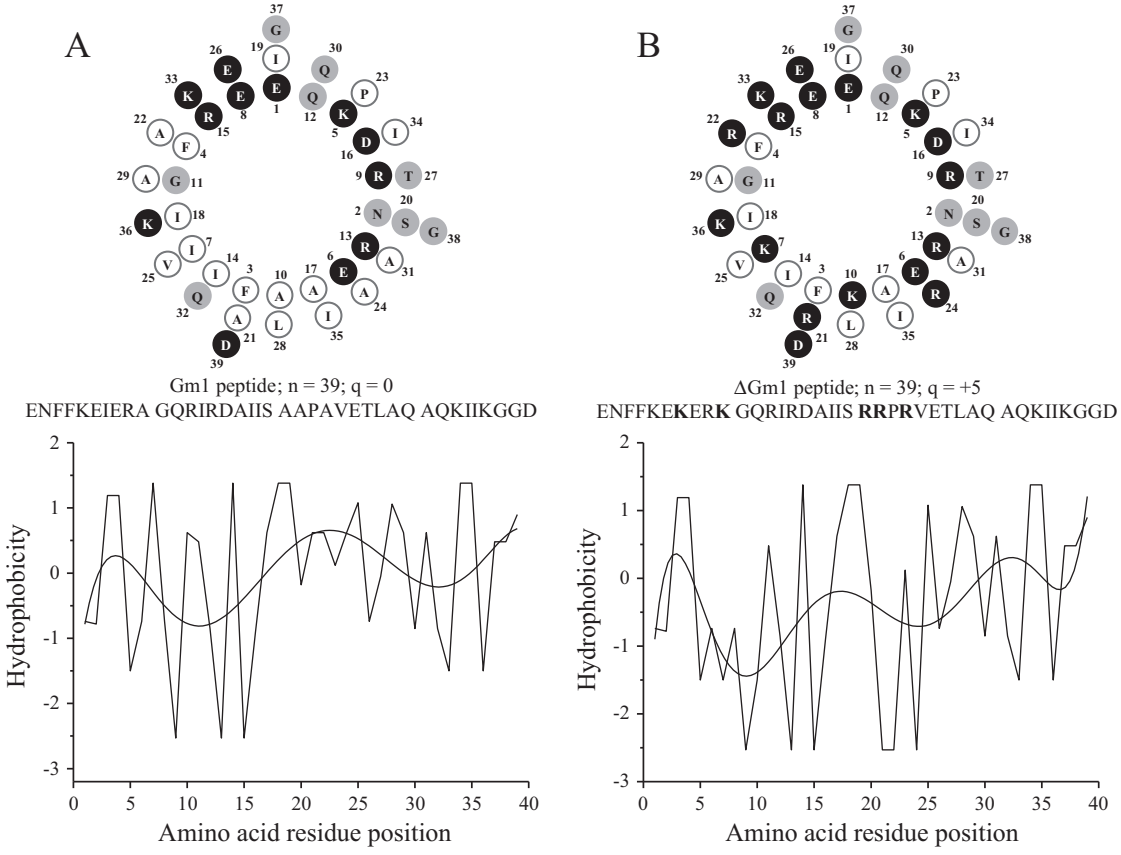

Fig. 1. Helical wheels and hydrophobicity plots of the peptides Gm1 (A) and ΔGm1 (B). Values were calculated using the consensus scale of hydrophobicities of Eisenberg et al. [21]. The sequences, lengths (n), and net charges (q) of Gm1 and ΔGm1 are shown. The exchange of aa in the sequence of Gm1 by cationic aa R and K in ΔGm1 are shown in bold.

evaluated (Fig. 2). For DMPG, bands at ~1220, 1168, 1098, 1067, and 1036 cm^{-1} could be detected, which can be assigned to the asymmetric PO_2^- stretching, asymmetric CO–O–C stretching, symmetric PO_2^- stretching, symmetric CO–O–C stretching and C–O–PO_2^- stretching vibration [36,37]. The bands at ~1201, 1177, and 1132 cm^{-1} can be assigned to the C–N stretching, CH_2 wagging vibration (γ_w), which are sensitive to hydrocarbon chain conformations, and Asp, Glu C–O stretching vibrations, respectively [33,38,39]. Table 1 shows a blue shift (shift to higher wavenumbers) of the ester carbonyl vibrational band C═O corresponding to low hydration in the interaction of Gm1 with DMPG and LPS R60, whereas the ΔGm1 peptide shifts the bands to lower wavenumbers (red shift). For the phosphate groups, an electrostatic interaction of these functional groups with Gm1 was found, while in the case of ΔGm1 no drastic changes were observed due to decrease of intensities of the spectra and overlapping bands. The shifts observed for the asymmetric C–O–PO_2^- stretching for both peptides and the changes of the band shapes for the phosphate vibrational bands are also important. These differences can be explained by sterical changes in the head group region (Fig. 2A). We could observe a shift in the asymmetric PO_2^- stretching and also changes of the band shapes when the peptides were incubated with LPS R60 (black arrows, Fig. 2B). These observations correlate directly with the influence of the peptides on the phase transition behavior of the lipids and also the fluidization and changes in T_m (see below).

The carbonyl stretching vibration of phospholipids has been studied extensively as a sensor for the hydration of lipid interface regions which

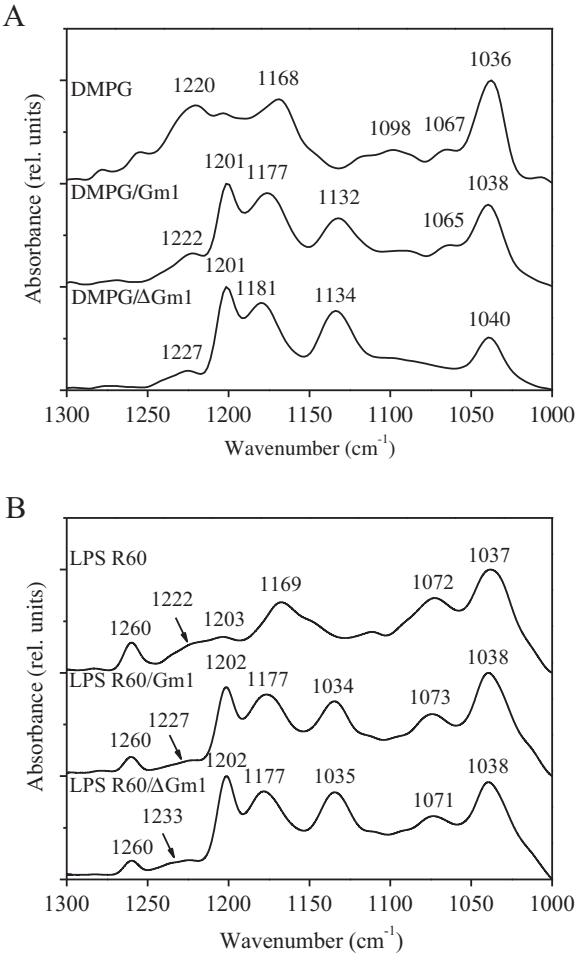

Fig. 2. Infrared ATR spectra of the head group stretching region for DMPG (A) and LPS R60 (B) with Gm1 and ΔGm1. The spectra of DMPG and LPS R60 were taken from a 10 mM hydrated film in HEPES buffer at pH 7.4 and 20 °C. The mixtures were prepared at a molar ratio of 1:0.5 [L]/[Peptides].

Table 1
Wavenumbers (cm^{-1}) of the component bands for C═O in DMPG and LPS R60 with peptides at a molar ratio of 1:0.5 [L]/[Peptides] as determined by Fourier self-deconvolution and band-shape simulation with Gaussian–Lorentzian functions.

	Carbonyl stretch (cm^{-1})	
	Low hydration	High hydration
DMPG	1740	1731
DMPG/Gm1 1:0.5	1744	1734
DMPG/ΔGm1 1:0.5	1738	1730
LPS R60	1730	1712
LPS R60/Gm1 1:0.5	1733	1716
LPS R60/ΔGm1 1:0.5	1731	1715

is sensitive to the hydration state, polarity, degree and nature of hydrogen bondings [40–43]. Clearly, the band at 1177 cm^{-1} was blue-shifted to 1181 cm^{-1} by the interaction with ΔGm1, indicating couples with adjacent CH_2 groups. The analyses of bands of ΔGm1 incubated with DMPG at different molar ratios (Fig. 2) showed a decrease of intensities of the bands assigned to DMPG and an increase of bands of ΔGm1. This agrees with an assignment of bands above. $\gamma_w CH_2$ displayed a red-shift until a molar ratio of 1:0.5. At this weight ratio the formation of microdomains reaches a point of maximum intercalation that depends on the initial head group–peptide interactions.

Tables 2, 3 and Fig. 3 summarizing the analysis of band patterns of different structural components of the peptides Gm1 and ΔGm1 with DMPG multilamellar vesicles (LMVs) and LPS R60 aggregates at a molar ratio of 1:0.5 lipid/peptide. These bands are characteristic for the secondary structures of the peptides. In particular, the amide I band is used to determine the secondary (alpha helical and beta sheet) conformations of proteins and peptides in lipid bilayers [35,44,45].

Gm1 displays band components at 1620 cm^{-1} and 1657 cm^{-1} corresponding to parallel β-sheets and helix structures respectively, and further band components' characteristic for unordered structures (random coils), turns and bends. In contrast, ΔGm1 did not exhibit an amount of *beta*-strands, but a band around 1638 cm^{-1}, indicating an antiparallel β-sheet. A high percentage of helix bands were located at 1655 cm^{-1}, but no unordered structures could be detected (Table 3). When the peptides were incubated with aggregates from DMPG and LPS R60, further band components as compared to the pure peptides occurred for ΔGm1 (Table 2). This observation was accompanied by a decrease in the percentage of helices, turns and bends and an increase in extended chains and unordered structures in the presence of LPS R60. For Gm1, no unordered components as well as turns and bends could be observed but the percentage of helices and extended chains increased (Table 3). These results are indicating significant changes of the secondary structures of the peptides when incubated with the lipid aggregates. In contrast, the position of the helix band of Gm1 shifted down by 3 cm^{-1} due to solvation of water molecules and an increase of the helix length [33]. The extended chains were more red-shifted, whereas there were no changes in wavenumbers of ΔGm1 with both lipids (Table 2).

3.3. Influence of peptides on the phase transition behavior of lipids by FTIR

The CH_2 stretching of the symmetric mode of the lipids acyl chain vibrational bands was analyzed for the elucidation of the gel to liquid crystalline phase behavior of the lipids [37,46]. Thus, the peak position of $\nu_s(CH_2)$ can be used to receive qualitative information about the amount of disorder in the hydrocarbon chains as well as to investigate thermotropic transitions of the lipid–peptide mixtures and possible demixing. The effect of Gm1 and ΔGm1 on the gel to liquid crystalline ($\beta \leftrightarrow \alpha$) phase transition of the hydrocarbon chains of DMPG LMVs and LPS R60 aggregates is shown in Fig. 4.

The influence of both peptides on the phase transition of DMPG is clearly expressed at all molar ratios. For Gm1 incubated with DMPG, a

Table 2
Amide I frequencies and assignments (cm^{-1}) by Fourier self-deconvolution and band-shape simulations with Gaussian–Lorentzian functions at a molar ratio of 1:0.5 [L]/[Peptides].

Peptides and [L]/[P] 1:0.5	Extended chains					Helix	Unordered	Turns and bends		
	Low wavenumber components				High wavenumber component					
Gm1				1620	1673	1657	1642		1685	1694
DMPG/Gm1		1638		1623	1674	1654				1695
LPSR60/Gm1		1637		1624	1679	1654		1670		1693
ΔGm1		1638		1622		1655		1670	1679	1694
DMPG/ΔGm1	1608	1637		1621	1677	1656		1669		1694
LPSR60/ΔGm1	1609		1633	1621	1679	1654	1642	1670		1694
Average	1609	1638	1633	1622	1676	1655	1642	1670	1682	1694
Deviation	0.7	0.6	0.0	1.5	2.8	1.3	0.0	0.5	4.2	0.6

fluidizing effect is observed at a molar ratio of 1:0.5 in both L_β (gel) and L_α (liquid crystalline) phases. This was accompanied by a decrease of the phase transition temperature (T_m) from ~25 °C to ~23 °C at a molar ratio of 1:0.1. A sharp phase transition vanishes completely at a molar ratio of 1:0.5, i.e., the peptide destabilizes both L_β and L_α, suggesting a disturbance of the acyl chain packing concomitant with a fluidization. In contrast, the T_m of ΔGm1 and DMPG increases considerably from ~25 °C to ~50 °C at a molar ratio of 1:1.0 with increasing rigidification (Fig. 4A,B).

In the case of LPS R60, Gm1 leads similarly as found for DMPG to a fluidizing of the negatively charged part of LPS, lipid A. The wavenumber increased in both phases which leads to the conclusion that the acyl chains of LPS R60 become much more disordered, however, a phase transition is still visible up to the highest peptide concentration. Again, in contrast is the behavior for the ΔGm1 LPS R60 interaction, T_m increases from ~38 °C to ~44 °C at the highest molar ratio, concomitant with nearly no changes of the wavenumber values (Fig. 4C,D).

3.4. Influence of peptides on the phase transition properties of lipids by DSC

Using calorimetry, changes in the stability of lipid phases in the presence of the peptides are very accurately determined. The main parameters obtained are the phase transition temperature and phase transition enthalpy [24]. DMPG shows in the presence of physiological ionic strength (ca. 140 mM NaCl, pH 7.4) two phase transitions. At ca. 12 °C the phase transition between two gel phases (L_β to P_β) and at ca. 23.3 °C the main phase transition liquid-crystalline ($\beta \leftrightarrow \alpha$). The presence of these phases depends on the solution conditions as ionic strength or pH, or the presence of extrinsic compounds [47]. The phase transition enthalpy of the main phase is 31 kJ/mol [25]. The presence of the peptides Gm1 and ΔGm1 has an impact on the presence of the P_β-phase. Fig. 5 shows exemplarily the thermograms (heat capacity curve) of DMPG in the presence of different ΔGm1 ratios. Already at DMPG to peptide ratio the low melting phase transition disappears and only one phase transition is observed. With increasing amount of ΔGm1 the phase transition enthalpy decreases and the phase transition temperature is shifted to higher temperatures. Fig. 6 summarizes the changes in phase transition temperature and enthalpy. The change in phase transition enthalpy is expressed in % of changes in order to be able to directly compare both lipids. At DMPG to ΔGm1 1:1 molar ratio the phase transition temperature is shifted to ca. 35 °C, thus indicating a stabilization of the gel phase. Analyzing the heat capacity curves it is also obvious with increasing amount of the peptide ΔGm1, that two phase transitions are observed. A first phase transition is observed at ca. 21–23 °C followed by a small exothermic peak, and a second phase transition at higher temperatures above 30 °C. The first phase transition is observed close to the phase transition of the pure main phase transition temperature of DMPG. Thus this phase transition can be related to the melting of a DMPG enriched phase. However, the second, high melting phase transition is likely to be due to a phase melting of a peptide enriched DMPG phase. Thus above DMPG to ΔGm1 1:0.5 molar ratio, one can assume phase separation into a DMPG rich and peptide rich phase.

In general, the phase transition enthalpy decreases with increasing amount of peptide. At a molar ratio of DMPG to ΔGm1 1:0.5 a shift in the phase transition temperature with an increase in phase transition enthalpy is observed, probably due to the formation of a peptide enriched DMPG phase. This is not observed for the other three lipid–peptide systems.

The gel phase of LPS R60 in the presence of ΔGm1 is also stabilized, but to a lower extent as observed for DMPG (Fig. 6A). With this a constant decrease in phase transition enthalpy is detected.

The presence of Gm1 on both lipids is however somewhat different. For both lipids a slight destabilization of the gel phase is detected, indicated by a decrease of the phase transition temperature. The impact on the phase transition temperature is however, not so pronounced as observed for the positively charged peptide ΔGm1.

Analyzing the phase transition enthalpy, decreases are observed (Fig. 6B), for DMPG-Gm1 at a molar ratio 1:1 the impact is so strong that no phase transition is observed in the temperature range of 5–95 °C. Fig. 6B shows that the impact of Gm1 on the phase transition temperature of both lipids is lower compared to ΔGm1, however, stronger changes in the phase transition enthalpy are detected.

Table 3
Structure percentages before and after lipid–peptide binding. The percentages of *beta*, turns and bend structures were calculated by adding the areas of all bands and expressing the sum as a fraction of the total amide I band areas, the same procedure was applied for helices and unordered structures. The errors are shown in parentheses.

Peptides and [L]/[P] 1:0,5	Extended chains	Helix	Unordered structures	Turns and bends
Gm1	24 (±0.7)	39 (±0.9)	32 (±0.8)	6 (±0.4)
DMPG/Gm1	57 (±0.9)	42 (±0.5)	0	1 (±0.8)
LPSR60/Gm1	37 (±1.4)	59 (±2.3)	0	4 (±0.1)
ΔGm1	35 (±1.5)	52 (±1.3)	0	13 (±1.2)
DMPG/ΔGm1	59 (±0.7)	37 (±0.2)	0	4 (±0.2)
LPSR60/ΔGm1	41 (±0.6)	30 (±0.2)	23 (±0.2)	6 (±0.5)

3.5. Intercalation of peptides into phospholipids and lipopolysaccharides by FRET spectroscopy

An intercalation of peptides into target membrane systems leads to a decrease of the energy transfer of the donor intensity (increase in donor intensity) and a decrease in acceptor intensity. Thus, the I_D/I_A ratio is a sensitive measure of incorporation. We analyzed their interaction with single liposomes consisting of phospholipids' characteristic of the cytoplasmic membranes of bacteria Gram-negatives (zwitterionic DMPE and negatively charged DMPG) and rough mutant LPS R595 and LPS R60 (Ra) by FRET. As demonstrated in Fig. 7, a similar incorporation at comparable lipid:peptide ratios is observed for all negatively charged lipids, i.e., for zwitterionic DMPE it is considerably lower. Interestingly, the two peptides do not differ significantly, this means that the overall charge distribution plays only a minor role in the intercalation process.

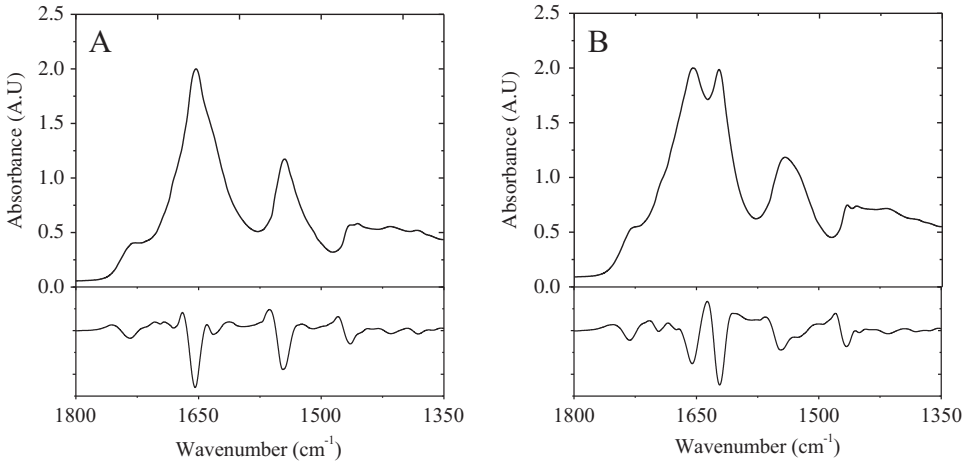

Fig. 3. Amides I, II and III ATR-FTIR spectra of Gm1 (A) and ΔGm1 (B) with LPS R60 and its amides I, II, III second derivatives. The spectra were taken at a lipid/peptide molar ratio of 1:0.5.

In the case of ΔGm1 and DMPG, there is a decrease in the signal from a certain concentration on (Fig. 7B), which can be explained by the developing of microdomains which exclude the dyes.

3.6. Thermodynamic analysis of the binding of Gm1 and ΔGm1 to LPS by ITC

The thermodynamics of the interaction of the two studied peptides Gm1 and ΔGm1 with two rough mutant LPS from *S. enterica* R60 and polymyxin B-resistant *P. mirabilis* R45 was investigated by isothermal titration calorimetry (ITC). The peptides were injected subsequently into the calorimeter cell containing only buffer (A) or the LPS dispersions at 37 °C. After each injection the enthalpy change was measured. As shown in Fig. 8B and C an exothermic binding interaction occurred for both peptides with LPS.

Importantly, there is a difference between the two LPS preparations with a lower exothermic enthalpy change for the LPS from the PMB-resistant R45 (Table 4). The reaction enthalpy of Gm1/LPS R60 is further decreased by α-helix formation (Table 3) since the conformational transition is an exothermic process. The binding of the peptides to the LPS aggregates is enthalpically and entropically driven, as reflected in the ΔH and −TΔS values (Table 4). Interestingly, there is no significant difference between the two peptides regarding the saturation values. For ΔGm1 with a positive charge of (+5), saturation takes place at nearly the same concentration ratio as for the overall uncharged Gm1 binding to LPS R60. Similar ΔG values were obtained for both peptides, this

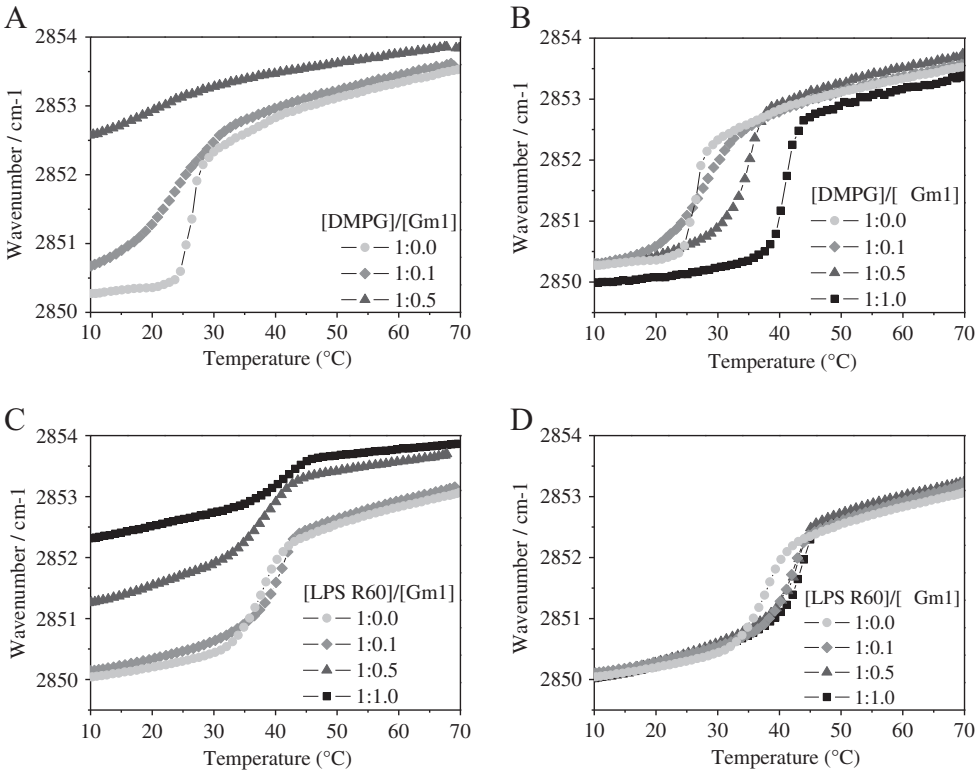

Fig. 4. Gel to liquid crystalline phase transition of the hydrocarbon chains of 10 mM preparations from DMPG and LPS R60 dispersions with Gm1 (A,C) and ΔGm1 (B,D) at different molar relations, respectively, from FTIR experiments. Presented is the peak position of the symmetric stretching vibrational band $\nu_s(CH_2)$ versus temperature. The gel phase lies around 2850 to 2850.5 cm^{-1}, while the liquid crystalline phase is in the range 2852.5 to 2853.0 cm^{-1}.

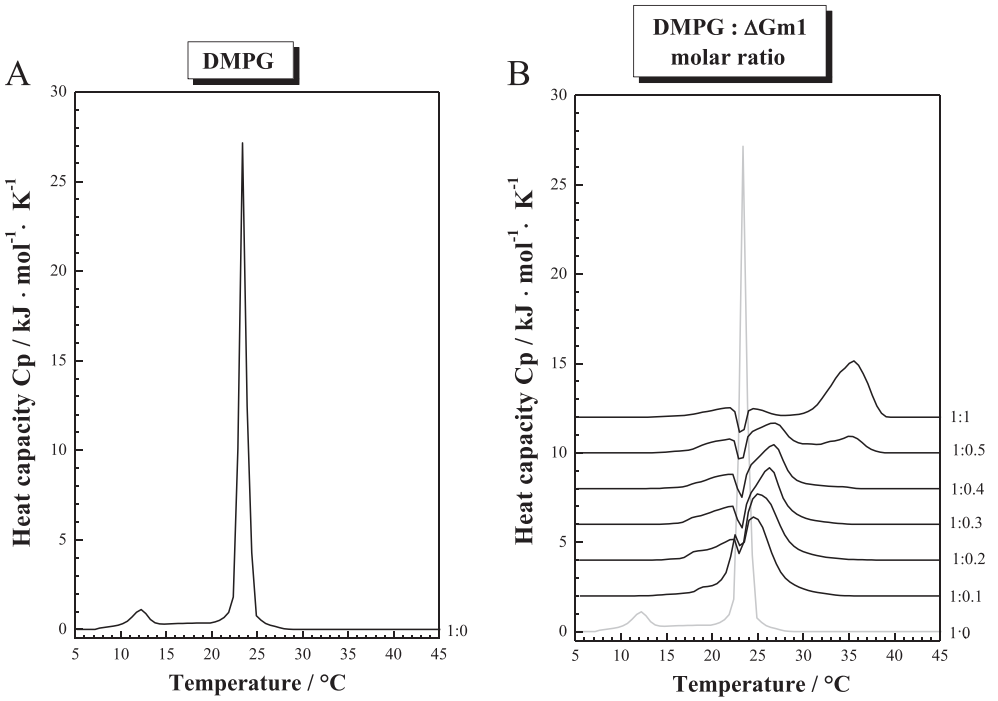

Fig. 5. Heat capacity curves of (A) pure DMPG and (B) various DMPG to ΔGm1 mixtures (molar ratio). Buffer: 10 mM PBS buffer at pH 7.4.

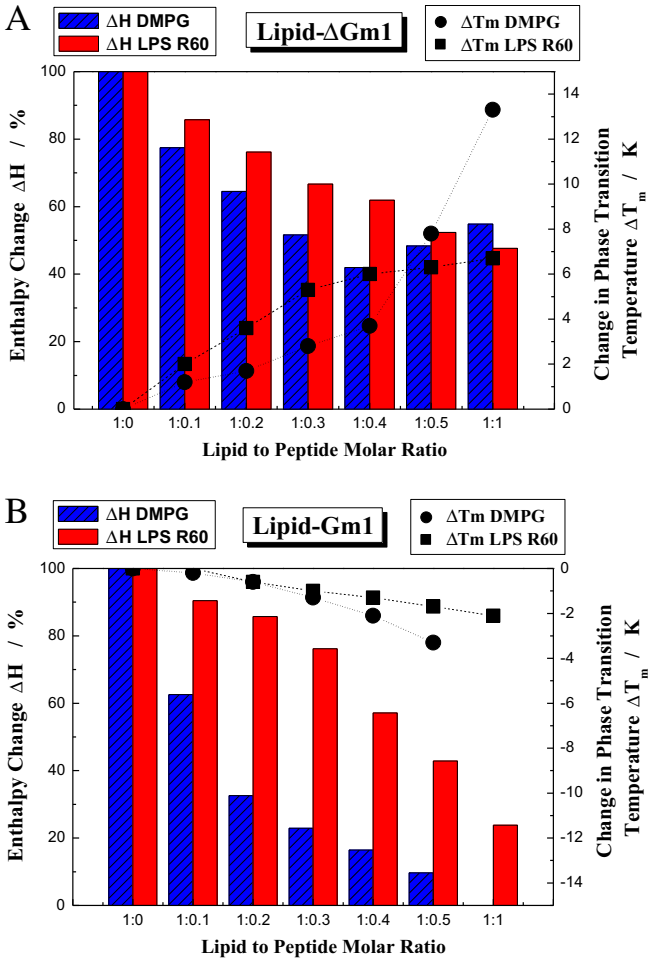

Fig. 6. Changes in phase transition enthalpy and temperature for DMPG and LPS R60 with ΔGm1 (A) and Gm1 (B) at various molar ratios, calculated from the measurement presented in Fig. 5.

can be explained by different structural formations on the interaction surface (Table 3) of the LPS aggregates, which can enhance the entropy and is thus a driving force towards binding.

4. Discussion

In the present study we examined the effect of Gm1 cecropin D-like peptide (Gm1) and its analogue ΔGm1 on selected membrane models in order to evaluate how these peptides interact with model compounds of the outer membranes of Gram-negative bacteria. One of the principal components of negatively charged bacterial phospholipids, DMPG, has been extensively studied in combination with anionic and zwitterionic lipids, concluding that cationic antimicrobial peptides are capable of promoting the formation of crystalline phases of DMPG and that a preference of peptides for these negatively charged head groups compared to other negatively charged phospholipids exists [48,49].

Applying the ATR/FTIR technique for elucidating interaction mechanisms of peptides with the lipid systems, the changes of vibrational bands of the lipids within the hydrophobic region, interfacial region and phosphate PO_2^- stretching modes can be monitored. Table 2 shows a comparative study of the influence of the two peptides on two of the basic negatively charged lipids of Gram-negative bacteria, DMPG and LPS R60. The position of the main band of the helix of Gm1 (~1657 cm^{-1}) shifts down concomitant with an increase in the percentage (39% to 42% and 59%) of the helix. The molecular structure of the helix leads to the best chemical solvation by water molecules or electrostatic interactions with cationic head groups which is important when the cecropins are interacting with membrane phospholipids. No red-shift of the helix was observed when this peptide interacted with DMPG and LPS R60, indicating that no deep insertion into the hydrophobic environment of the membrane takes place. An opposed effect could be observed by Morgera et al. [50], using the human helical peptide LL-37 characterized by a high content of both cationic and anionic residues. The decrease in the percentage of unordered, turns and bend structures was accompanied by an increase of β-sheet structures and also a red-shift of this band. This indicates that Gm1 changes its structure by interacting with the hydrophilic region of the membrane head groups, followed by increasing its helix length, which seems to

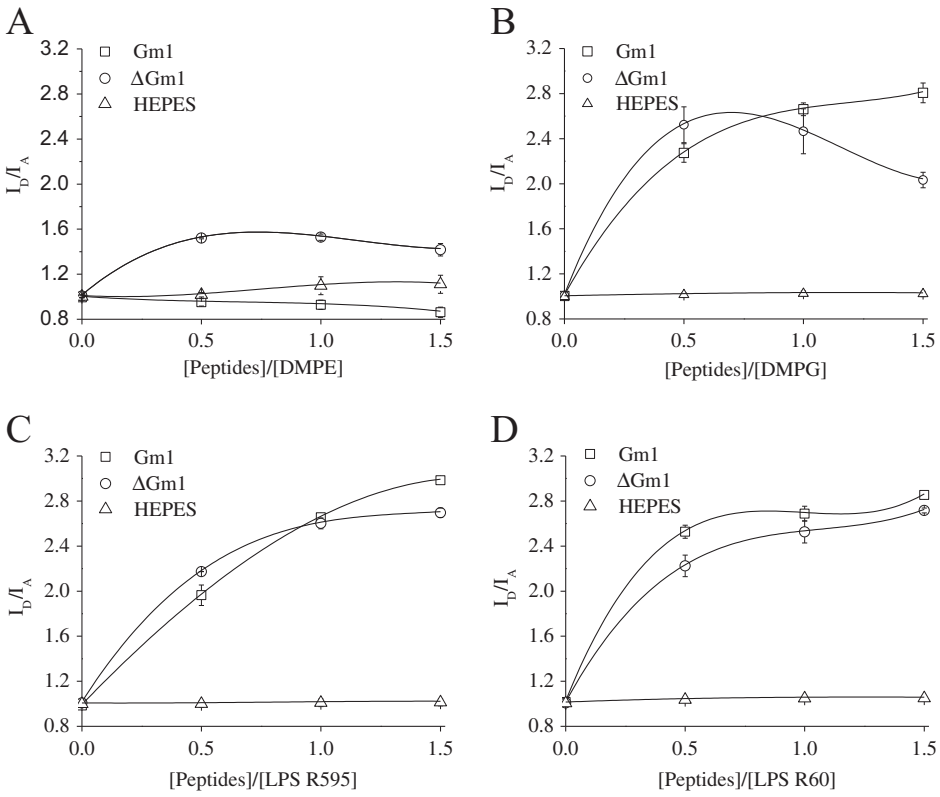

Fig. 7. The FRET signal I_D/I_A is plotted against [Peptide]/[Lipid or lipopolysaccharide] molar ratio upon the addition of 10 μL of Gm1 and ΔGm1 (0.5 mM) to 1000 μL of equimolar mixtures (0.1 mM) of double-labeled lipids composed of single DMPE (A), DMPG (B), LPS R595 (C) and LPS R60 (D), and HEPES as a control. The molar ratios [L]/[P] are shown for each point.

correspond to the data found for magainins or cecropins [51]. ΔGm1 did not change the wavenumbers in the amide I region when this peptide was incubated with DMPG and LPS R60, but the secondary structure components showed different percentages of the single secondary structures as compared to the pure peptide. The increase of β-structures with both membranes and the increase in disorder induced in LPS R60 aggregates are indicative of the initial electrostatic interaction between anionic head groups and peptides.

The increase in FRET efficiency led to an increase of the $I_{Donor}/I_{Acceptor}$ ratio, suggesting that both peptides were intercalated into the model membranes by locating themselves into the lipid head group regions with subsequent insertion. Interestingly, after 5 min (molar ratio [DMPG]/[ΔGm1] = 0.5) the I_D/I_A decreased, indicating the formation of superficial peptide-enriched microdomains which led to the exclusion of the dyes. Apparently there is no basic difference in the intercalation ability of the two peptides, despite the fact that they differ largely in the number of charges. This is in agreement with results presented earlier with cyclic peptides based on the *Limulus* anti-LPS factor [52,53], and with linear peptides constructed to optimally binding the lipid A portion of LPS [54]. The FRET signal (ratio of donor to acceptor emission intensity) of DMPE liposomes is much lower than the signals for DMPG and LPS (Fig. 7), which emphasizes the importance of negatively charged compounds of bacterial membranes for a binding with antimicrobial compounds. Also, the nearly identical intercalation of the two peptides into LPS with differing sugar chain lengths (LPS R595, short sugar; LPS R60 long sugar) is indicative of the importance of the lipid A moiety of LPS for the interaction process, which is in accordance to the fact that the lengths of the sugar chains within LPS preparations may play a role for the integrity of the bacterial cells, but not for the interaction processes with external compounds [55].

The effect exerted by Gm1 on the gel to liquid-crystalline ($\beta \leftrightarrow \alpha$) phase transition, leading to a fluidization (Fig. 4A, C), similar as found for the action of polymyxin B on negatively charged lipids [56]. This can be interpreted by a membrane binding and intercalation, resulting in a deep penetration of the peptide into the hydrophobic core of the bilayers formed by DMPG and LPS R60. It is indicated by a decrease of the phase transition enthalpy (Figs. 5, 6).

These disturbances of the acyl chain packing and fluidization are consistent with the red-shift of the β-sheet structures observed when Gm1 was incubated with both lipids, possibly leading to the formation of membrane lesions. At first glance, the data for ΔGm1 in Figs. 4 and 7 seem to be contradictory. However, the intercalation seen in the FRET experiment of DMPG with decreasing signal at higher peptide concentration (Fig. 7) indicates an exclusion of the dye and/or the precipitation of the complex, which would be completely compatible with the rigidification (Fig. 4, wavenumber values decreasing from 2852.5 to 2850.4 cm^{-1}) in the FTIR experiment. Such precipitation is not seen for the LPS:ΔGm1 systems (Fig. 4), which correlates with the observation that the rigidification of LPS at 37 °C (Fig. 4) is only marginal.

The increase in the acyl chain state of order of bilayers from DMPG and LPS at all molar ratios ΔGm1 (rigidifying effect) is probably due to a superficial binding to the membrane. The observed shifts in T_m can be explained by the ability of the peptides to induce a perturbation in the bilayers which leads to a change in the thermodynamic parameters related to the phase transition [40]. This kind of interaction can increase the mean distance between adjacent lipids molecules without penetrating the acyl chain region. This is also in accordance with the increase in FRET efficiency and the shift in amide I bands associated with insertion into the hydrophobic environment.

The evaluation of the infrared spectra of the head group region of the lipids provides a more precise characterization of the interaction, the decrease of the intensities of phosphate groups can be attributed to a reduction of their mobility. The interaction of ΔGm1 with DMPG and LPS R60 was stronger than the interaction with Gm1 deduced from the changes of the band shapes, which is concomitant with immobilization of the phosphates. The blue-shifts in asymmetric PO_2^- and $C-O-PO_2^-$ stretching vibrational bands (Fig. 2) are indicating that a change to a more positively charged peptide (ΔGm1) increases the interaction

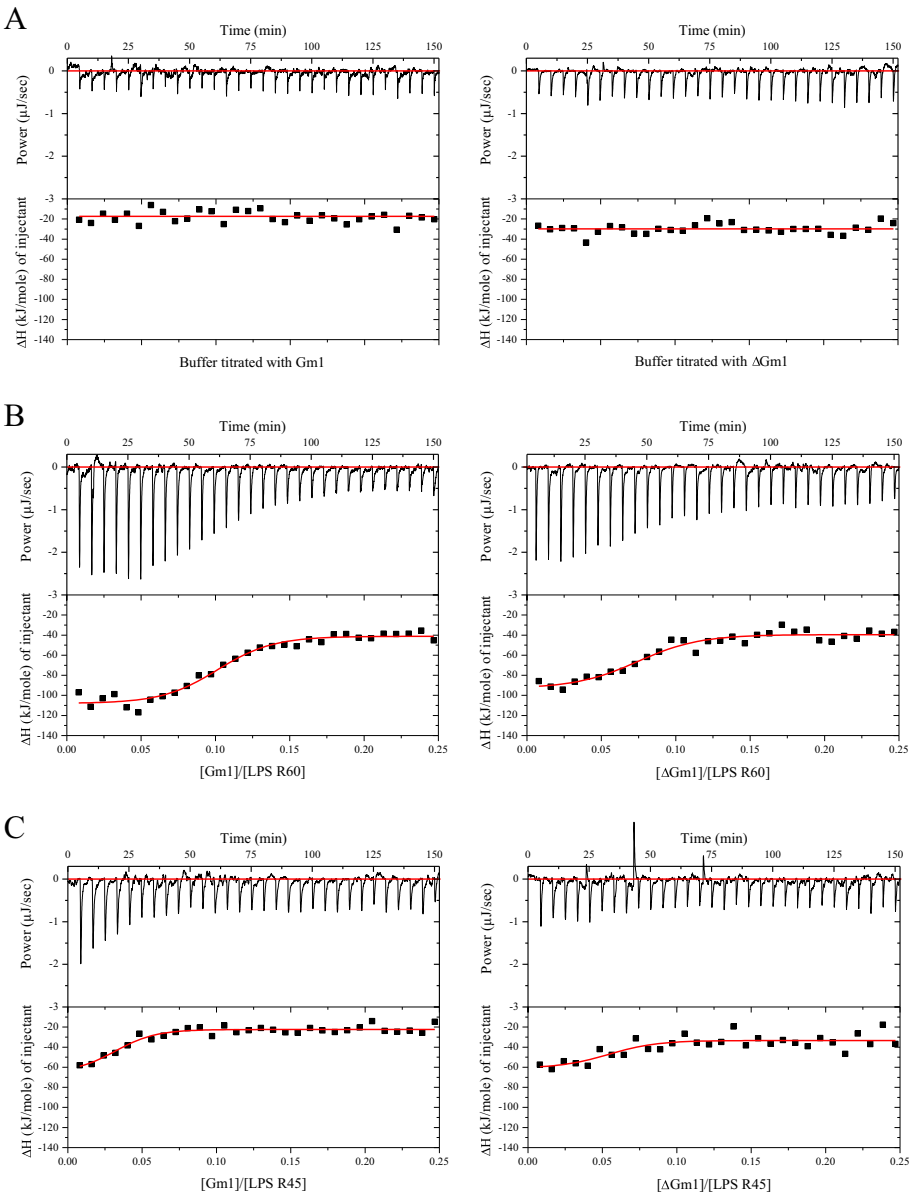

Fig. 8. Isothermal titration calorimetry of Gm1 and ΔGm1 into pure buffer (A), and into LPS R60 (B) and LPS R45 (C) dispersions at 37 °C. The peptides were either titrated into pure buffer or into the LPS dispersions and the heat was recorded, the lower curves represent the heat of the reaction measured by peak integration as a function of peptide/LPS molar ratio, with concentration of peptides being 0.2 mM and of LPS 0.05 mM. The solid lines represent the best fits to experimental data and the thermodynamic parameters calculated from these experiments are presented in Table 4.

with the membrane head groups. In order to understand this behavior, the shifts can be interpreted as changes in the order and orientation of water molecules in the hydration shell of the head groups, because the interaction of the positive amino acid (aa) residues with the negatively charged head groups breaks the ordered water layer, modifying the electrostatic properties of the lipids, which can explain also the shifts in the T_m of DMPG and LPS R60 to higher temperatures. T_m depends to a certain extent on the structure of the polar head-groups. Therefore, ΔGm1 induces a disordered packing in the polar head-group region by modifying the surface-bond water molecules and affecting the cooperativity of the lipids which react with increasing order of the acyl chains. When looking onto the LPS sugar chain region,

Table 4
Thermodynamic parameters for Gm1 and ΔGm1 binding to LPS R60 and LPS R45 aggregates at 37 °C. n, represents the stoichiometry of the interaction.

Peptide/LPS	n	K_A (M^{-1})	ΔG (kJ/mol)[a]	ΔH (kJ/mol)	ΔS (kJ/mol/K)[b]
Gm1/R60	0.10	$1.23 \times 10^5 \pm 1.80 \times 10^4$	−30.17 ± 0.38	−13.22 ± 1.83	0.05 ± 0.01
Gm1/R45	0.04	$1.19 \times 10^5 \pm 2.62 \times 10^4$	−30.60 ± 0.17	−3.63 ± 1.88	0.09 ± 0.01
ΔGm1/R60	0.08	$1.30 \times 10^5 \pm 3.32 \times 10^4$	−29.73 ± 0.07	−4.68 ± 1.73	0.08 ± 0.01
ΔGm1/R45	Nd	Nd	Nd	−2.48 ± 0.42	Nd

Nd: not determined.
[a] Free energy was calculated according to $\Delta G = -RT\ln K_A$.
[b] The entropy of binding was calculated with $\Delta G = \Delta H - T\Delta S$.

no shift or even a disappearance was observed for the sugar bands at 1030–1040 cm^{-1} or 1070–1090 cm^{-1}, which is indicative of a low affinity or no binding of the peptides to the sugar backbone. Dathe et al. [57,58] demonstrated that binding to and insertion into membranes are determined by a balance of electrostatic attraction to the lipid head groups and hydrophobic interaction with the bilayer core. When the attraction between positively charged residues on the hydrophilic face of the peptide helix and the lipid head groups is enhanced by the addition of anionic lipids to the bilayers, the peptide is associated more tightly to the head group region of the lipid bilayers and its penetration into the hydrophobic core is reduced. Our results are consistent with this model in which the interaction of ΔGm1 resulted in an increased perturbation of head groups, leading to a rigidifying effect. In addition to this, Gm1 displayed a stronger binding to the interfacial region in both model membranes, whereas ΔGm1 had only an effect on the carbonyl stretches associated to hydrogen bonds (Table 1). The shifts observed in $\gamma_w CH_2$ (Fig. 2) are the result of a rearrangement of the structure of ΔGm1 (Table 3) which leads to the formation of enriched peptide–lipid microdomains as a result of the interaction. Remarkably are the thermodynamic data of the Gm peptides binding to the LPS aggregates exhibiting exothermic reactions due to Coulomb interactions of the positively charged aa of the peptides with the negative charges of the lipids, independently of the detailed charge distribution within the peptide aa sequences. This means that a polycationic character alone as found for other AMP [59] is not necessary a prerequisite for effective binding. This observation is in accordance to findings of the binding of lipopolyamines, which are polar but not necessarily positively charged compounds, to LPS, which leads also to an exothermic reaction with high affinity [60]. Importantly, the reduced ΔH of the interaction of both peptides with the PMB-resistant LPS R45 compared to the sensitive LPS R60 (Fig. 8, Table 4) indicates that the additional positively charged 4-amino-4-deoxy-L-arabinoses linked to the 4′-phosphate group and to the first 2-keto-3-deoxyoctonate unit of the inner core of LPS R45 in varying quantities [61], which are absent in the LPS R60 affect the binding. They represent a sterical hindrance as well as a charge shifting to a less negatively charged LPS molecule. As also described for PMB this leads to a reduced interaction capability, because the peptides cannot pass to their target phosphate groups.

5. Conclusions

The presented data demonstrated the importance of the analysis from the details of the interaction mechanisms between antimicrobial peptides and negatively charged bacterial surface structures on a molecular level. As an interpretation, the displacement of water molecules in the hydration shell by electrostatic interactions of cationic residues of the peptides with phosphate head groups of both lipids leads to changes in their three-dimensional structure with strong consequences for the membrane properties. The increase of disorder of the acyl chains by deep penetration of Gm1 led to the formation of membrane-inserted domains, and it could be speculated that this may be connected with the release of intracellular components. In contrast, the results for the lysine-arginine rich peptide ΔGm1 showed that an increase of the charge number (0 to +5) led to a superficial binding to the membranes with a special affinity for polar head groups. In the following paper, we will focus our investigations on the antibacterial and anti-endotoxin properties of the two Gm peptides to characterize their possible ability as drug against severe infections.

Acknowledgements

Wilmar Correa wishes to thank Nina Hahlbrock, Christine Hamann and Carlotta Ober-Blöbaum for the introduction to analytic techniques and help. We also are grateful to the peptide synthesis group (Rainer Bartels and Volker Grote). This work was supported by German Ministry BMBF (project 01GU0824), Else-Kröner-Fresenius-Stiftung (project A_140, 2011), Universidad de Antioquia (CODI IN618CE, and Estrategia de Sostenibilidad 2011–2012) and Programa Enlaza Mundos Alcaldía de Medellín-(No. 0892-21 de Octubre de 2011).

References

[1] A.C. Engler, N. Wiradharma, Z.Y. Ong, D.J. Coady, J.L. Hedrick, Y.-Y. Yang, Emerging trends in macromolecular antimicrobials to fight multi-drug-resistant infections, Nano Today 7 (2012) 201–222.
[2] K. Brandenburg, P. Garidel, S. Fukuoka, J. Howe, M.H.J. Koch, T. Gutsmann, J. Andrä, Molecular basis for endotoxin neutralization by amphipathic peptides derived from the α-helical cationic core-region of NK-lysin, Biophys. Chem. 150 (2010) 80–87.
[3] M. Zasloff, Antimicrobial peptides of multicellular organisms, Nature 415 (2002) 389–395.
[4] K.A. Brogden, Antimicrobial peptides: pore formers or metabolic inhibitors in bacteria? Nat. Rev. Microbiol. 3 (2005) 238–250.
[5] N. Papo, Y. Shai, Can we predict biological activity of antimicrobial peptides from their interactions with model phospholipid membranes? Peptides 24 (2003) 1693–1703.
[6] R.M. Epand, H.J. Vogel, Diversity of antimicrobial peptides and their mechanisms of action, Biochim. Biophys. Acta 1462 (1999) 11–28.
[7] K.L. Brown, R.E.W. Hancock, Cationic host defense (antimicrobial) peptides, Curr. Opin. Immunol. 18 (2006) 24–30.
[8] R.E.W. Hancock, H.-G. Sahl, Antimicrobial and host-defense peptides as new anti-infective therapeutic strategies, Nat. Biotechnol. 24 (2006) 1551–1557.
[9] E. Guaní-Guerra, T. Santos-Mendoza, S.O. Lugo-Reyes, L.M. Terán, Antimicrobial peptides: general overview and clinical implications in human health and disease, Clin. Immunol. 135 (2010) 1–11.
[10] J.M. Sanderson, Peptide–lipid interactions: insights and perspectives, Org. Biomol. Chem. 3 (2005) 201–212.
[11] R.E.W. Hancock, K.L. Brown, N. Mookherjee, Host defence peptides from invertebrates — emerging antimicrobial strategies, Immunobiology 211 (2006) 315–322.
[12] R.E.W. Hancock, D.S. Chapple, Peptide antibiotics, Antimicrob. Agents Chemother. 43 (1999) 1317–1323.
[13] S.E. Brown, A. Howard, A.B. Kasprzak, K.H. Gordon, P.D. East, A peptidomics study reveals the impressive antimicrobial peptide arsenal of the wax moth *Galleria mellonella*, Insect Biochem. Mol. Biol. 39 (2009) 792–800.
[14] M. Andrejko, M. Mizerska-Dudka, T. Jakubowicz, Antibacterial activity in vivo and in vitro in the hemolymph of *Galleria mellonella* infected with *Pseudomonas aeruginosa*, Comp. Biochem. Physiol. B Biochem. Mol. Biol. 152 (2009) 118–123.
[15] I. Wojda, P. Kowalski, T. Jakubowicz, Humoral immune response of *Galleria mellonella* larvae after infection by *Beauveria bassiana* under optimal and heat-shock conditions, J. Insect Physiol. 55 (2009) 525–531.
[16] P. Mak, A. Zdybicka-Barabas, M. Cytryńska, A different repertoire of *Galleria mellonella* antimicrobial peptides in larvae challenged with bacteria and fungi, Dev. Comp. Immunol. 34 (2010) 1129–1136.
[17] M. Cytryńska, P. Mak, A. Zdybicka-Barabas, P. Suder, T. Jakubowicz, Purification and characterization of eight peptides from *Galleria mellonella* immune hemolymph, Peptides 28 (2007) 533–546.
[18] T. Gutsmann, U. Seydel, Impact of the glycostructure of amphiphilic membrane components on the function of the outer membrane of Gram-negative bacteria as a matrix for incorporated channels and a target for antimicrobial peptides or proteins, Eur. J. Cell Biol. 89 (2010) 11–23.
[19] M.P. Bos, J. Tommassen, Biogenesis of the Gram-negative bacterial outer membrane, Curr. Opin. Microbiol. 7 (2004) 610–616.
[20] R.P.H. Huijbregts, A.I.P.M. de Kroon, B. de Kruijff, Topology and transport of membrane lipids in bacteria, Biochim. Biophys. Acta 1469 (2000) 43–61.
[21] D. Eisenberg, E. Schwarz, M. Komaromy, R. Wall, Analysis of membrane and surface protein sequences with the hydrophobic moment plot, J. Mol. Biol. 179 (1984) 125–142.
[22] C. Galanos, O. Lüderitz, O. Westphal, A new method for the extraction of R lipopolysaccharides, Eur. J. Biochem. 9 (1969) 245–249.
[23] J.L.R. Arrondo, F.M. Goñi, Infrared studies of protein-induced perturbation of lipids in lipoproteins and membranes, Chem. Phys. Lipids 96 (1998) 53–68.
[24] P. Garidel, A. Blume, Miscibility of phospholipids with identical headgroups and acyl chain lengths differing by two methylene units: effects of headgroup structure and headgroup charge, Biochim. Biophys. Acta 1371 (1998) 83–95.
[25] P. Garidel, A. Blume, Miscibility of phosphatidylethanolamine–phosphatidylglycerol mixtures as a function of pH and acyl chain length, Eur. Biophys. J. 28 (2000) 629–638.
[26] A.B. Schromm, K. Brandenburg, E.T. Rietschel, H.-D. Flad, S.F. Carroll, U. Seydel, Lipopolysaccharide-binding protein mediates CD14-independent intercalation of lipopolysaccharide into phospholipid membranes, FEBS Lett. 399 (1996) 267–271.
[27] K. Brandenburg, J. Andrä, T. Gutsmann, J. Howe, P. Garidel, Isothermal titration calorimetric studies of the interaction of phospho- and glycolipids with anti-effective agents, in: L. Denes, A. Kiado (Eds.), Thermal Analysis in Medical Application (Wide Diversity in Thermal Analysis and Calorimetry), vol. 1, Akadémiai Kiadó, Budapest, 2011, pp. 37–60.
[28] K. Brandenburg, A. David, J. Howe, M.H.J. Koch, J. Andrä, P. Garidel, Temperature dependence of the binding of endotoxins to the polycationic peptides polymyxin B and its nonapeptide, Biophys. J. 88 (2005) 1845–1858.
[29] D. Bordo, P. Argos, Suggestions for "safe" residue substitutions in site-directed mutagenesis, J. Mol. Biol. 217 (1991) 721–729.
[30] J.W. Bryson, S.F. Betz, H.S. Lu, D.J. Suich, H.X. Zhou, K.T. O'Neil, W.F. DeGrado, Protein design: a hierarchic approach, Science 270 (1995) 935–941.

[31] J.K. Myers, C.N. Pace, J.M. Scholtz, Helix propensities are identical in proteins and peptides, Biochemistry 36 (1997) 10923–10929.
[32] A. Roy, A. Kucukural, Y. Zhang, I-TASSER: a unified platform for automated protein structure and function prediction, Nat. Protoc. 5 (2010) 725–738.
[33] A. Barth, Infrared spectroscopy of proteins, Biochim. Biophys. Acta 1767 (2007) 1073–1101.
[34] P.I. Haris, D. Chapman, The conformational analysis of peptides using fourier transform IR spectroscopy, Biopolymers 37 (1995) 251–263.
[35] L.K. Tamm, S.A. Tatulian, Infrared spectroscopy of proteins and peptides in lipid bilayers, Q. Rev. Biophys. 30 (1997) 365–429.
[36] W. Hübner, A. Blume, Interactions at the lipid–water interface, Chem. Phys. Lipids 96 (1998) 99–123.
[37] A. Blume, Properties of lipid vesicles: FT-IR spectroscopy and fluorescence probe studies, Curr. Opin. Colloid Interface Sci. 1 (1996) 64–77.
[38] H. Nakahara, S. Lee, O. Shibata, Specific interaction restrains structural transitions of an amphiphilic peptide in pulmonary surfactant model systems: an in situ PM-IRRAS investigation, Biochim. Biophys. Acta 1798 (2010) 1263–1271.
[39] A. Barth, The infrared absorption of amino acid side chains, Prog. Biophys. Mol. Biol. 74 (2000) 141–173.
[40] M.M. Moreno, P. Garidel, M. Suwalsky, J. Howe, K. Brandenburg, The membrane-activity of Ibuprofen, Diclofenac, and Naproxen: a physico-chemical study with lecithin phospholipids, Biochim. Biophys. Acta 1788 (2009) 1296–1303.
[41] C. Selle, W. Pohle, Fourier transform infrared spectroscopy as a probe for the study of the hydration of lipid self-assemblies. II. Water binding versus phase transitions, Biospectroscopy 4 (1998) 281–294.
[42] A. Blume, W. Huebner, G. Messner, Fourier transform infrared spectroscopy of 13 C═O labeled phospholipids hydrogen bonding to carbonyl groups, Biochemistry 27 (1988) 8239–8249.
[43] W. Pohle, C. Selle, H. Fritzsche, H. Binder, Fourier transform infrared spectroscopy as a probe for the study of the hydration of lipid self-assemblies. I. Methodology and general phenomena, Biospectroscopy 4 (1998) 267–280.
[44] E. Goormaghtigh, V. Raussens, J.-M. Ruysschaert, Attenuated total reflection infrared spectroscopy of proteins and lipids in biological membranes, Biochim. Biophys. Acta 1422 (1999) 105–185.
[45] D.M. Byler, H. Susi, Examination of the secondary structure of proteins by deconvolved FTIR spectra, Biopolymers 25 (1986) 469–487.
[46] H.H. Mantsch, R.N. McElhaney, Phospholipid phase transitions in model and biological membranes as studied by infrared spectroscopy, Chem. Phys. Lipids 57 (1991) 213–226.
[47] P. Garidel, C. Johann, A. Blume, Thermodynamics of lipid organization and domain formation in phospholipid bilayers, J. Liposome Res. 10 (2000) 131–158.
[48] R.F. Epand, L. Maloy, A. Ramamoorthy, R.M. Epand, Amphipathic helical cationic antimicrobial peptides promote rapid formation of crystalline states in the presence of phosphatidylglycerol: lipid clustering in anionic membranes, Biophys. J. 98 (2010) 2564–2573.
[49] A. Arouri, M. Dathe, A. Blume, Peptide induced demixing in PG/PE lipid mixtures: a mechanism for the specificity of antimicrobial peptides towards bacterial membranes? Biochim. Biophys. Acta 1788 (2009) 650–659.
[50] F. Morgera, L. Vaccari, N. Antcheva, D. Scaini, S. Pacor, A. Tossi, Primate cathelicidin orthologues display different structures and membrane interactions, Biochem. J. 417 (2009) 727–735.
[51] R.M. Epand, R.F. Epand, Lipid domains in bacterial membranes and the action of antimicrobial agents, Biochim. Biophys. Acta 1788 (2009) 289–294.
[52] J. Andrä, M. Lamata, G. Martinez de Tejada, R. Bartels, M.H.J. Koch, K. Brandenburg, Cyclic antimicrobial peptides based on Limulus anti-lipopolysaccharide factor for neutralization of lipopolysaccharide, Biochem. Pharmacol. 68 (2004) 1297–1307.
[53] J. Andrä, J. Howe, P. Garidel, M. Rössle, W. Richter, J. Leiva-Leon, I. Moriyon, R. Bartels, T. Gutsmann, K. Brandenburg, Mechanism of interaction of optimized *Limulus*-derived cyclic peptides with endotoxins: thermodynamic, biophysical and microbiological analysis, Biochem. J. 406 (2007) 297–307.
[54] Y. Kaconis, I. Kowalski, J. Howe, A. Brauser, W. Richter, I. Razquin-Olazarán, M. Iñigo-Pestaña, P. Garidel, M. Rössle, G. Martinez de Tejada, T. Gutsmann, K. Brandenburg, Biophysical mechanisms of endotoxin neutralization by cationic amphiphilic peptides, Biophys. J. 100 (2011) 2652–2661.
[55] K. Brandenburg, A. Wiese, Endotoxins: relationships between structure, function, and activity, Curr. Top. Med. Chem. 4 (2004) 1127–1146.
[56] K. Brandenburg, I. Moriyon, M.D. Arraiza, G. Lewark-Yvetot, M.H.J. Koch, U. Seydel, Biophysical investigations into the interaction of lipopolysaccharide with polymyxins, Thermochim. Acta 382 (2002) 189–198.
[57] M. Dathe, H. Nikolenko, J. Meyer, M. Beyermann, M. Bienert, Optimization of the antimicrobial activity of magainin peptides by modification of charge, FEBS Lett. 501 (2001) 146–150.
[58] M. Dathe, T. Wieprecht, Structural features of helical antimicrobial peptides: their potential to modulate activity on model membranes and biological cells, Biochim. Biophys. Acta 1462 (1999) 71–87.
[59] T. Gutsmann, I. Razquin-Olazarán, I. Kowalski, Y. Kaconis, J. Howe, R. Bartels, M. Hornef, T. Schürholz, M. Rössle, S. Sanchez-Gómez, I. Moriyon, G. Martinez de Tejada, K. Brandenburg, New antiseptic peptides to protect against endotoxin-mediated shock, Antimicrob. Agents Chemother. 54 (2010) 3817–3824.
[60] D. Sil, L. Heinbockel, Y. Kaconis, M. Rössle, P. Garidel, S.A. David, K. Brandenburg, Insights into the neutralization of endotoxins by lipopolyamines, Open Biochem. J. 7 (2013) 83–93.
[61] T. Schuerholz, S. Domming, M. Hornef, A. Dupont, I. Kowalski, Y. Kaconis, L. Heinbockel, J. Andra, P. Garidel, T. Gutsmann, S. David, S. Sanchez-Gomez, G. Martinez de Tejada, K. Brandenburg Bacterial, Cell wall compounds as promising targets of antimicrobial agents II. Immunological and clinical aspects, Curr. Drug Targets 13 (2012) 1131–1137.